Microbiological Research 268 (2023) 127297

Contents lists available at ScienceDirect

Microbiological Research

journal homepage: www.elsevier.com/locate/micres

The quorum sensing *com* system regulates pneumococcal colonisation and invasive disease in a pseudo-stratified airway tissue model

Christian R. Kahlert [a,b], Susanne Nigg [a], Lucas Onder [c], Ronald Dijkman [d], Liliane Diener [e], Ana G. Jop Vidal [f], Regulo Rodriguez [g], Pietro Vernazza [a], Volker Thiel [h,i], Jorge E. Vidal [f,1], Werner C. Albrich [a,*,1,2]

[a] Division of Infectious Diseases & Hospital Epidemiology, Cantonal Hospital St. Gallen, Switzerland
[b] Children's Hospital of Eastern Switzerland, Infectious Disease & Hospital Epidemiology, St. Gallen, Switzerland
[c] Institute of Immunobiology, Cantonal Hospital St. Gallen, Switzerland
[d] Institute for Infectious Diseases, University of Bern, Bern, Switzerland
[e] Empa, Swiss Federal Laboratories for Materials Science and Technology, St. Gallen, Switzerland
[f] Department of Cell and Molecular Biology, and Center for Immunology and Microbial Research, University of Mississippi Medical Center, Jackson, MS, USA
[g] Institute of Pathology, Cantonal Hospital St. Gallen, Switzerland
[h] Institute of Virology and Immunology, Bern, Switzerland
[i] Department of Infectious Diseases and Pathobiology, Vetsuisse Faculty, University of Bern, Bern, Switzerland

ARTICLE INFO

Keywords:
Pneumococcus
Pathogenesis
Quorum sensing
Human bronchial epithelial cell culture model
Colonisations
Invasion

ABSTRACT

Background:: The effects of the *com* quorum sensing system during colonisation and invasion of *Streptococcus pneumoniae* (Spn) are poorly understood.
Methods: We developed an *ex vivo* model of differentiated human airway epithelial (HAE) cells with beating ciliae, mucus production and tight junctions to study Spn colonisation and translocation. HAE cells were inoculated with Spn wild-type TIGR4 (*wtSpn*) or its isogenic Δ*comC* quorum sensing-deficient mutant.
Results: Colonisation density of Δ*comC* mutant was lower after 6 h but higher at 19 h and 30 h compared to *wtSpn*. Translocation correlated inversely with colonisation density. Transepithelial electric resistance (TEER) decreased after pneumococcal inoculation and correlated with increased translocation. Confocal imaging illustrated prominent microcolony formation with wtSpn but disintegration of microcolony structures with ΔcomC mutant. ΔcomC mutant showed greater cytotoxicity than wtSpn, suggesting that cytotoxicity was likely not the mechanism leading to translocation. There was greater density- and time-dependent increase of inflammatory cytokines including NLRP3 inflammasome-related IL-18 after infection with Δ*comC* compared with wtSpn. ComC inactivation was associated with increased pneumolysin expression.
Conclusions: ComC system allows a higher organisational level of population structure resulting in microcolony formation, increased early colonisation and subsequent translocation. We propose that ComC inactivation unleashes a very different and possibly more virulent phenotype that merits further investigation.

1. Introduction

Community-acquired pneumonia due to *Streptococcus pneumoniae* (Spn) is associated with high morbidity and mortality worldwide (Welte et al., 2012). Currently there are at least 100 different pneumococcal serotypes known with different ability to cause mucosal and invasive pneumococcal disease (IPD) (Ganaie et al., 2020). Colonisation with subsequent carriage in the upper airways is considered a "conditio sine qua non" for the development of pneumococcal respiratory tract infections and IPD (Bogaert et al., 2004; Scott et al., 2012). A critical colonisation density in the nasopharynx above which there is a high risk for pneumococcal pneumonia versus asymptomatic colonisation has been demonstrated in adults and children (Albrich et al., 2012; Boix-Palop et al., 2021; Carr et al., 2021).

* Corresponding author.
E-mail addresses: christian.kahlert@kispisg.ch (C.R. Kahlert), werner.albrich@kssg.ch (W.C. Albrich).
[1] equal contributions.
[2] Presented in part: ISPPD 12, 19-23 June 2022, Toronto, Ca. Oral presentation, abstract: # 379.

https://doi.org/10.1016/j.micres.2022.127297
Received 10 August 2022; Received in revised form 22 December 2022; Accepted 27 December 2022
Available online 31 December 2022
0944-5013/© 2022 The Author(s). Published by Elsevier GmbH. This is an open access article under the CC BY-NC-ND license (http://creativecommons.org/licenses/by-nc-nd/4.0/).

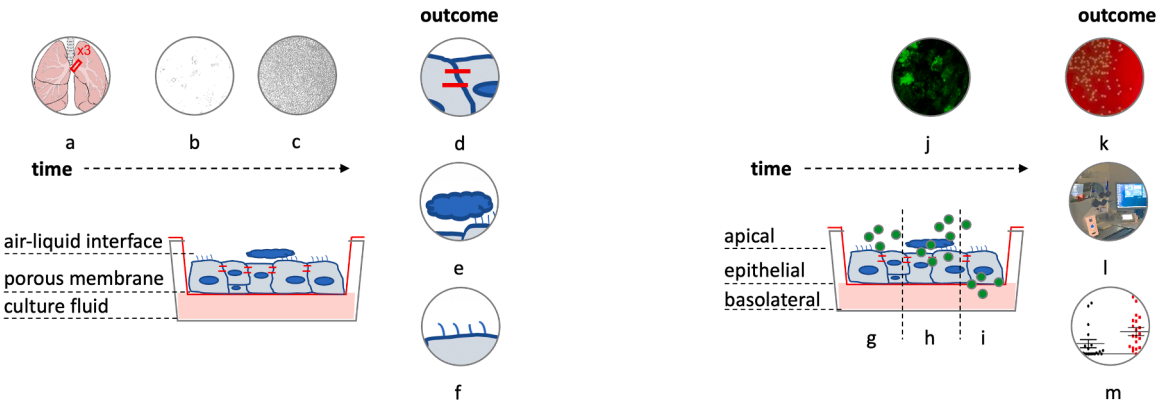

Fig. 1. *Modelling pneumococcal invasive disease: from colonisation (apical) to transmigration and translocation (basolateral).* Left, *non-infected model*. Primary human bronchial epithelial cells were isolated from bronchial biopsy samples from 5 donors (a). Cells were transferred as a single cell suspension (b) to a transwell insert that contains a membrane with pore size of 1 μm and incubated with culture medium in both the apical and basolateral side. Cells were incubated until the formation of a confluent monolayer when the cell culture medium was removed from the apical side to expose cells to air (air-liquid interface). Incubation was continued until the establishment of a differentiated pseudostratified bronchial epithelium (c) with tight junctions (d) mucus production (e), ciliary activity (f). Right, *infected model.* To simulate the in-vivo pathogenesis and assess colonisation (g) and epithelial adhesion, transmigration (h) through the epithelium and finally translocation to the basolateral side ("invasive pneumococcal disease", i), the established epithelium was inoculated on the apical side with different strains of *Streptococcus pneumoniae* (j) at 15 or 30 multiplicity of infection (MOI) and infected cells were incubated for 6 h, 19 h or 30 h. Finally, 3 different spaces (apical, epithelial, basolateral) were evaluated as follows: Pneumococci in the apical and basolateral side were cultured (k), cytotoxicity of the epithelium was assessed by obtaining the transepithelial electrical resistance (TEER), the release of lactate dehydrogenase (LDH) as well as by confocal microscopy (l). In addition, the epithelial response to pneumococcus was evaluated for the release of cytokines and zonulin-1 (m) including the corresponding mRNA expression.

Spn encodes and produces different quorum sensing (QS) systems including the *com* QS system. Recent studies showed that Com regulates colonisation and biofilm production on human lung and pharyngeal cells (Vidal et al., 2013a). Com, encoded by the locus *comABCD*, regulates expression of genes which are involved in competence-induced bacterial killing and fratricide, production of lantibiotics (Phr peptide QS), and increased virulence due to increased production of capsular polysaccharides (Trappetti et al., 2017). Despite years of investigation in the field, and the known importance of the Com for the biology of pneumococcus, the role of Com in invasion and translocation -the hallmark of pneumococcal invasive disease- has not been investigated yet and it represents an important gap in our understanding of pneumococcal pathogenesis.

To study pneumococcal-human interaction, animal models and immortalised cell culture models are generally utilised. The latter frequently consists of cancer cell lines, which represent an "artificial" environment lacking natural tissue diversity, differentiation and functionality (e.g. mucus production) of involved specialised airway cells and the 3D structure of the human lung epithelium, including the physiological air-liquid interface (ALI) and formation of tight-junctions (TJs) (Chiavolini et al., 2008; Hocke et al., 2017). Recently, an experimental human Spn carriage model has been developed (Gritzfeld et al., 2013; Felice et al., 1987; Wright et al., 2013). 24 h after individuals were infected with Spn serotype 6B strain, a different cytokine response was observed in those who were colonised by Spn compared to those infected but cleared the infection (Nikolaou et al., 2021). Whereas the human carriage model is helpful for carriage and vaccine studies, for ethical reasons studies on pneumococcal virulence and lung pathogenesis are challenging in human volunteers.

An *ex vivo* tissue model of primary human airway epithelial cells (HAE) with an air-liquid interface (ALI) was recently developed to study coronavirus pathogenesis (Dijkman et al., 2013a). This model includes a pseudo-stratified HAE cell layer containing basal, secretory, columnar, and ciliated cell populations. Thus, the *ex vivo* system recapitulates essential aspects of human airway epithelia, namely (i) presence of well-defined human airway epithelial cell types, which become (ii) functional and differentiated by producing mucus and showing ciliary activity, and (iii) maintains physico-biochemical barriers, such as the mucus layer, and a well-formed TJ belt with development of a trans-epithelial electrical resistance (TEER). These advantageous physiological characteristics and absence of an *ex vivo* model of human lung infection motivated us to adopt this *ex vivo* HAE-ALI model. We therefore infected differentiated human lung cells with a reference Spn strain TIGR4 (wildtype) or its isogenic Δ*comC* mutant and comprehensively compared colonisation, invasion, translocation, cytotoxicity, and human lung epithelial cell response.

2. Material and methods

2.1. Differentiated respiratory epithelium

Bronchial epithelial cells were isolated from bronchial biopsy samples of 5 different human donors with a median age of 70 years and cryopreserved as previously described (Dijkman et al., 2013a). This was done in accordance with local regulations from Cantonal Hospital St. Gallen, Switzerland, St. Gallen Lung Biopsy Biobank (SGLBB) with approval by the ethics committee of the Canton St. Gallen (EKSG 11/044). Bronchial epithelial cells were cultured in flat bottom 12-well plates (Greiner bio-one, Switzerland) on an insert covered by a membrane with 1 μm pores until formation of a confluent differentiated epithelial monolayer with beating cilia and mucus production at the ALI apical side. Cells were counted to 500'000 per insert by flow cytometry (BD FACSCANTO II, Becton Dickinson, United States). This process was monitored by TEER measurement until a stable mean resistance was reached.

2.2. Pneumococcal infection

Spn strains were inoculated in a 200 μl suspension of balanced salt solution (BSS, for detailed composition, see supplemental file) on the apical side at different multiplicity of infection (MOI). ALI medium (Fulcher et al., 2005) was added to the basolateral side. Pneumococci colonizing the apical compartment or invasive Spn in the basolateral compartment were counted by dilution and plating onto blood agar plates (measured as cfu/ml). Inactivated TIGR4 or latex particles served as negative controls.

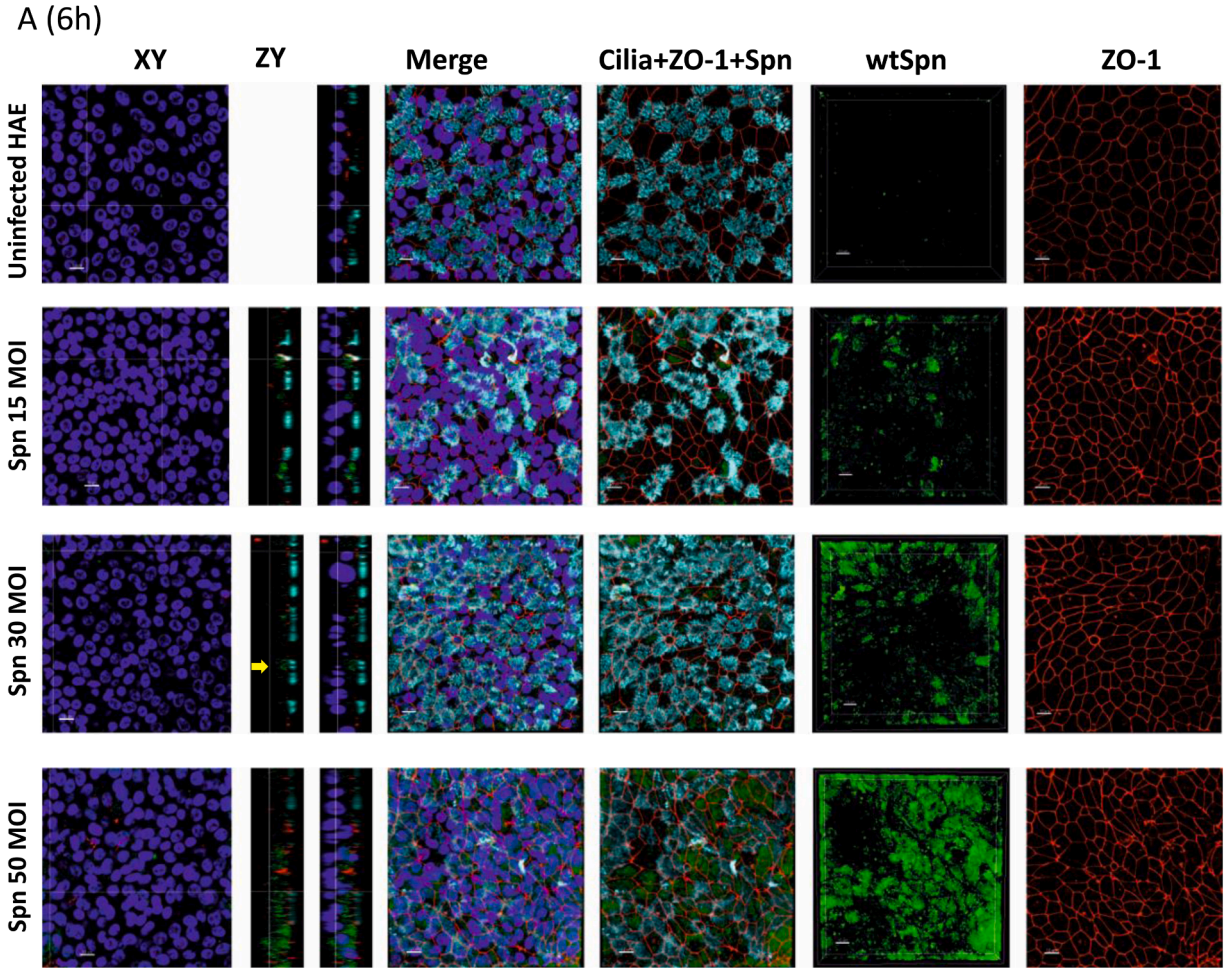

Fig. 2. Confocal microscopy of human airway epithelial (HAE) cell cultures infected with wtSpn and ΔcomC mutant. HAE cells infected with wtSpn or Δ*comC* mutant are shown after 6 h (A, B), 19 h (C, D) and 30 h (E, F) post-inoculation. Within each panel (A-F), the top row shows uninfected HAE cells, the second row HAE cells infected with 15 MOI, the third row HAE cells infected with 30 MOI and the fourth row shows HAE cells infected with 50 MOI of pneumococci. Immunostaining, indicated on top of each panel, was performed with DAPI (4′,6-diamidino-2-phenylindole) for nuclei, monoclonal antibodies against anti-β-tubulin IV to detect ciliated cells (light blue), against ZO-1 for tight junctions (red) and fluorescein-conjugated antibody against *S. pneumoniae* (green, indicated at TIGR4 or Δ*comC*). Columns depict stacks in XY plain or where indicated, orthogonal ZY plain. The panels in the XY plain provide a view from the top of the respective insert at the level shown in the ZY plain. This has to be taken into account when comparing signal intensities between different panels. For precise quantifications, we refer to Fig. 3. Yellow arrow shows pneumococci underneath both cilia staining and ZO-1 signal. The preparations were examined with confocal microscopy. Bars in all panels= 10 μm.

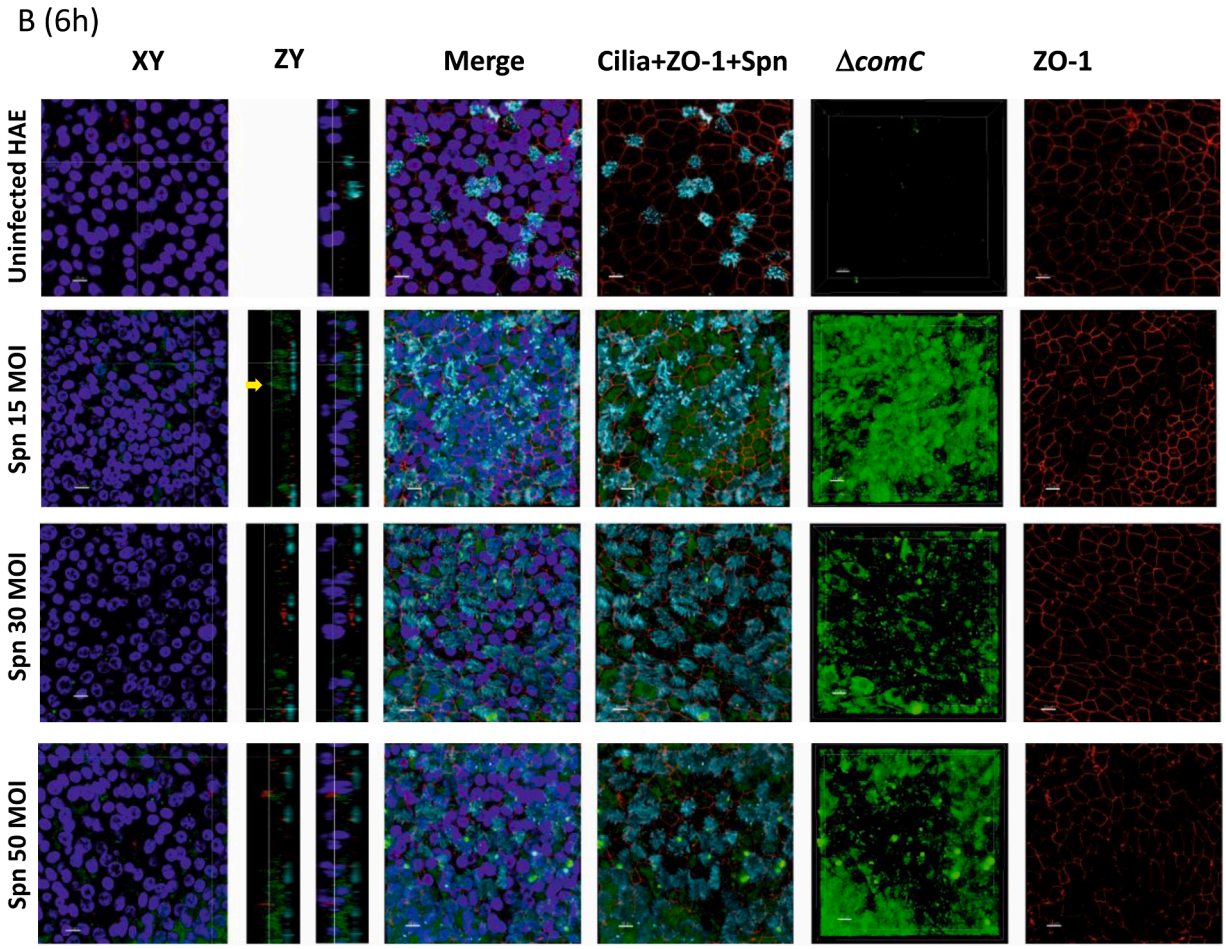

Fig. 2. (*continued*).

2.3. Bacterial strains

Pneumococcal strains were grown in Todd Hewitt broth containing 0.5% (w/v) yeast extract (THY) media at 37 °C and 5% CO2 until they reached a phase of logarithmic growth. For most experiments wild-type (wt) encapsulated serotype 4 TIGR4 strain (labelled as wtSpn, unless specified otherwise) or an isogenic TIGR4ΔcomC mutant (Vidal et al., 2013b) was used to study the influence of the Com quorum sensing system. Growth curves for wtSpn and ΔcomC mutant were similar (supplemental Fig. 1A). Both bacterial strains were further compared regarding four additional properties. Comparable results were obtained for both strains in terms of H_2O_2 production (supplemental Fig. 1B). Western blot and haemoglobin release assay (as a measure of Ply-induced hemolysis) revealed that the Δ*comC* mutant produced more pneumolysin (Ply) than the wtSpn under the culture conditions assessed in this study (supplemental Figs. 1C and 1D). Confocal microscopy and flow cytometry assays demonstrated similar expression of serotype 4 capsular antigen in both strains (supplemental Figs. 1E and 1F). Further details on the methods used can be found in the supplemental file.

2.4. Confocal microscopy analysis

Confocal imaging analysis was performed as a non-quantitative method to visualize the ultrastructure of the epithelium and the localization location of pneumococci during colonisation, invasion and translocation. Infected HAE cultures were fixed with 4% paraformaldehyde (PFA) for 30 min at room temperature, followed by rinsing of the apical and basolateral sides three times with 1 ml of phosphate-buffered saline (PBS). Fixed HAE cultures were immunostained using a previously described procedure (Dijkman et al., 2013b). Briefly, images were captured using a Zeiss LMS 710 confocal microscope (Zeiss, Jena, Germany) and analyzed and processed using IMARIS Version 7.7.2 (Oxford Instruments, Bitplane AG, Zürich, Switzerland).

2.5. Trans-epithelial electrical resistance (TEER)

To measure the integrity of TJ in the epithelial monolayers, TEER measurement (in Ω/cm2) was performed using the Epithelial Volt/Ohm (TEER) Meter (EVOM2®, World Precision Instruments, Sarasota, FL, United States) in different donors according to the manufacturer's instructions. The first measured TEER level was set at 100% as a baseline and TEER measurements over time were calculated as percentage of baseline values. To avoid cross-contamination when obtaining bacterial counts from the apical and basolateral compartments, separate inserts were used for TEER measurement.

2.6. Cytokine detection by multiplex ELISA cytokine array and quantitative PCR

Inflammatory cytokines were measured in the supernatant by a multiplex ELISA array (Eve Technologies, Calgary, Canada). In addition, mean mRNA expression was measured relative to β -actin from the lysate

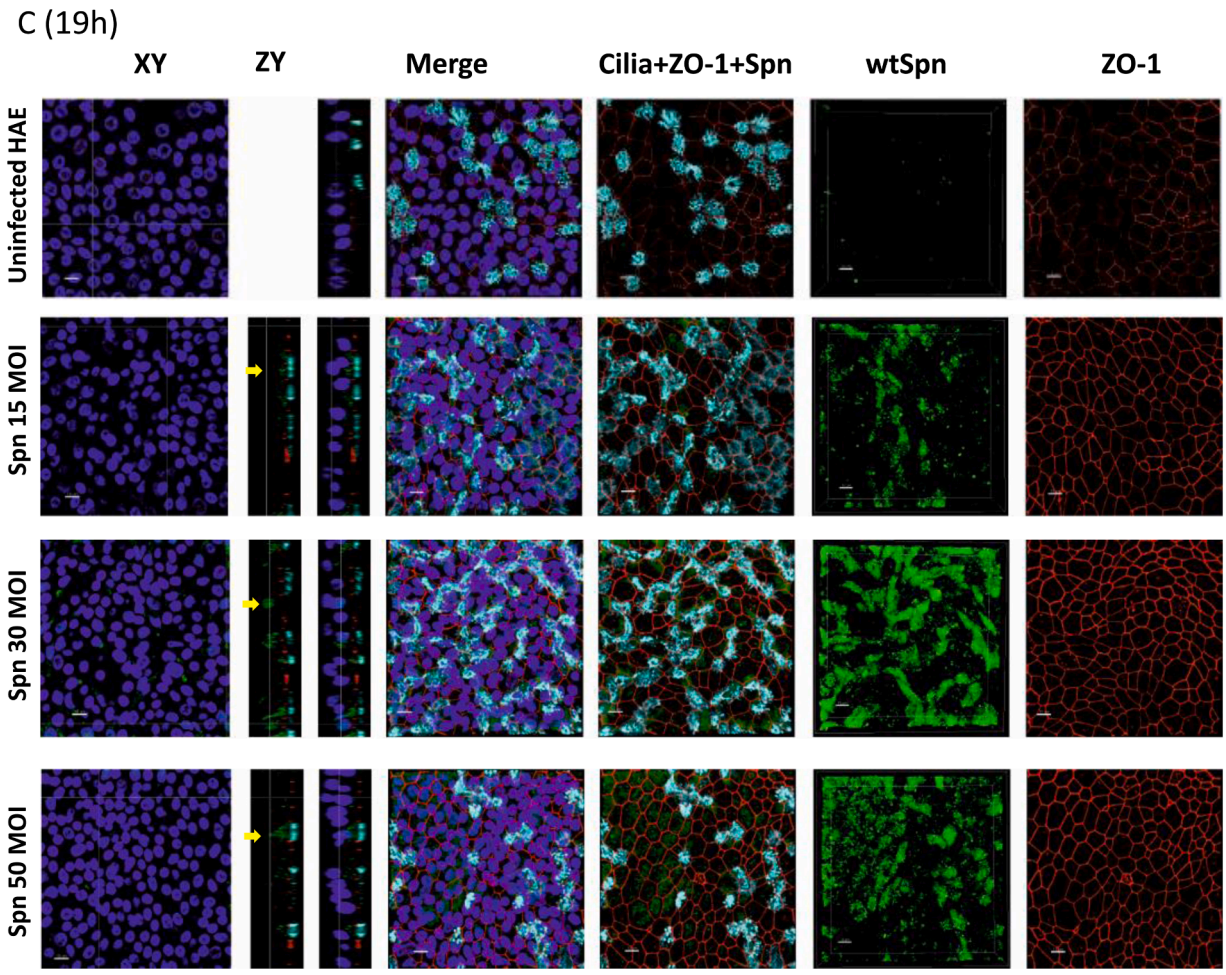

Fig. 2. (*continued*).

of the epithelium as inflammatory host response.

2.7. Zonulin-1 detection by ELISA and quantitative PCR

Zonulin-1 (ZO-1) expression was measured in the supernatant by an ELISA array (My BioSource, Unites States). In addition, total RNA was extracted (RNeasy® Mini Kit, Qiagen, Netherlands) after homogenization of the lysate of the epithelium using QIAshredder® (Qiagen, Netherlands). Subsequently, mean mRNA expression was measured relative to β-actin (QuantStudio® 5, Applied Biosystems, United States). The β-actin primer (forward AGC CTC GCC TTT GCC GA and reverse CTG GTG CCT GGG GCG) as well as probe (5' Hex CCG CCG CCC GTC CAC ACC CGC C and 3' BHQ-1) sequences were utilized.

2.8. Cytotoxicity

Lactate dehydrogenase (LDH), which is released during cell lysis, was measured in supernatant as a marker of cytotoxicity using the colorimetric non-radioactive cytotoxicity assay CytoTox96® according to the manufacturer's instructions (Promega, Madison, WI, United States). Cytotoxicity was measured in supernatant from HAE cells with and without infection with wildtype and ΔcomC. BSS was used as negative control. As an assay positive control, HAE cells were incubated with lysis solution as indicated by the manufacturer. Results were read using a photometer Tecan Sunrise® (Tecan, Männedorf, Switzerland) at OD490. To quantify LDH release in the supernatant, a standard curve was produced with serial dilutions of purified LDH provided in the kit, diluted in phosphate-buffered saline (PBS) + 1% bovine serum albumin (BSA). The concentration of LDH was measured using Konelab 60 (Thermofischer, Switzerland). The standard curve spanned from 500 U/ml through 15 U/ml, the latter considered the limit of detection. A linear regression analysis was performed and used to calculate the concentration in the supernatants. To assess whether lactate LDH was released from epithelial cells or pneumococcus during an infection experiment we measured LDH release from Spn in the absence of HAE cells. For this purpose, Spn at 15 MOI were placed in BSS without culture medium and without HAE cells on a membrane with 0.4 μm pore size.

2.9. Flow cytometry

Non-infected HAE cells from two donors were taken from culture, washed and trypsinised to a single cell suspension. 10^4 cells were stained using three fluorescent-labelled antibodies (CD326 APC, CD31 PE and 7AAD PerCP-Cy5). Cells were acquired by flow cytometry (FACSCanto, Becton, Dickinson and Company, United States) and fibroblasts were defined as negative for CD326 or CD31 (see supplemental Fig. 2).

2.10. Transmission electron microscopy

Cells were cultivated as described previously and treated with 50 MOI Spn for 19 h at 37 °C and 5% CO_2. Cells were fixed in 3% glutaraldehyde in 0.1 M sodium cacodylate buffer and were washed in 0.2 M sodium cacodylate buffer. After a post-fixation step in 2% osmium tetroxide in 0.1 M sodium cacodylate buffer, samples were dehydrated

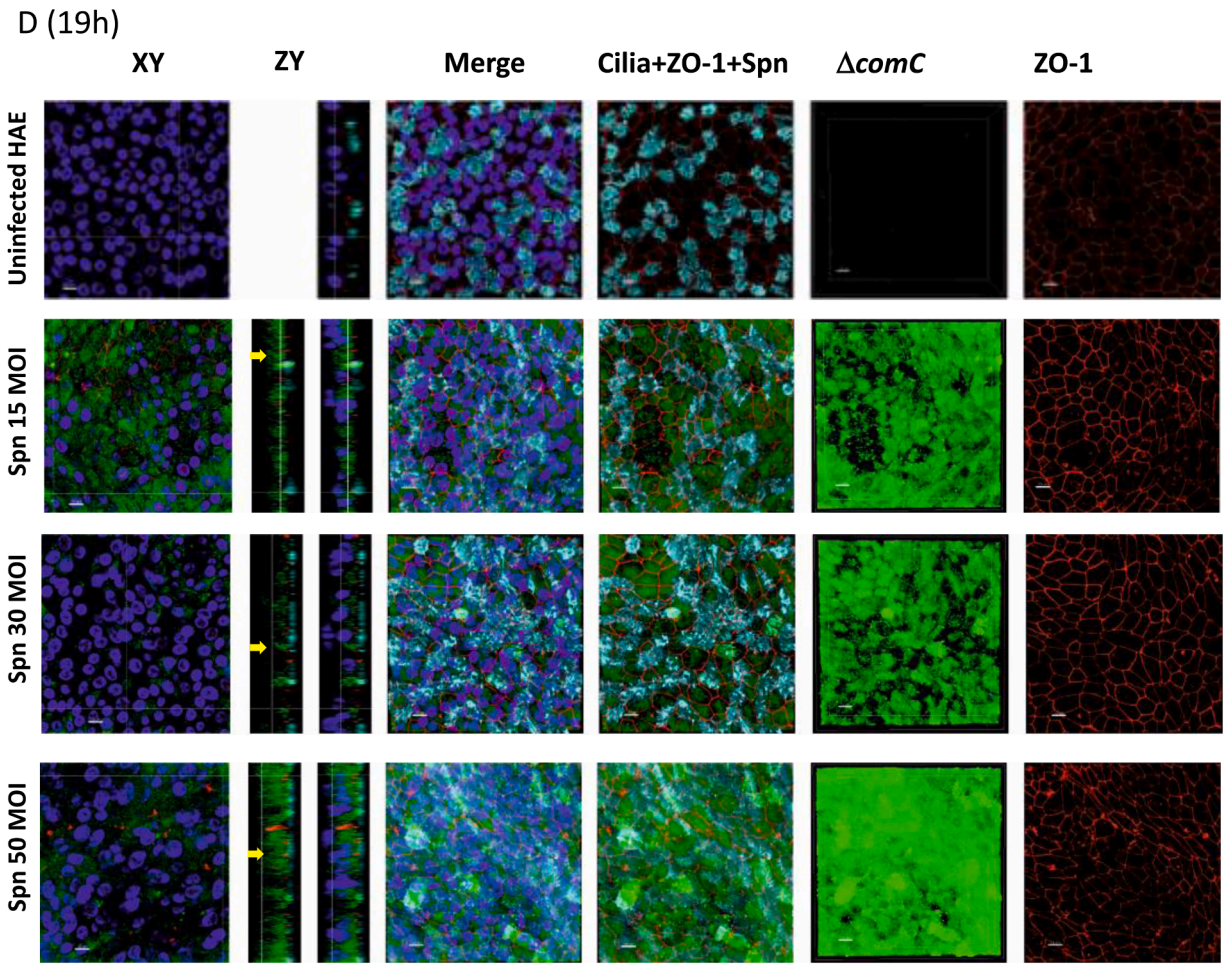

Fig. 2. (*continued*).

through a graded ethanol series followed by acetone and finally embedded in Epon resin (Sigma-Aldrich, Buchs, Switzerland). Ultrathin sections were contrasted with 2% uranyl acetate and lead citrate (Reynolds 1963) before imaged in a Zeiss EM 900 (Carl Zeiss Microscopy GmbH, Germany) at 80 kV.

2.11. Statistical analysis

Continuous variables were compared using the Mann-Whitney U test or non-paired t-test, as appropriate. Time course of TEER measurements was compared between different doses of the same strain using Spearman correlation coefficients. The dose- and time-dependent differences of TEER measurements between two strains were analyzed using 3-way analysis of variance (ANOVA) using donor as block factor. Statistical analyses were performed using Prism (GraphPad Software, San Diego, CA, United States) and R (Vienna, Austria). P-values < 0.05 were considered statistically significant.

3. Results

3.1. Primary HAE cells differentiate ex-vivo upon exposure to air

To model pneumococcal colonisation and invasive disease, cells from five different donors were cultured (Fig. 1). Integrity, and differentiation upon exposure to air [i.e., beating cilia (supplemental Movie 1–3), and mucus production] was observed by traditional *light microscopy* (Fig. 1). Confocal imaging showed ciliated structures and formation of a well-defined TJ complex, as evidenced by the presence of zonulin-1 (Fig. 2, ZO-1 in control cells). We confirmed by *flow cytometry* that HAE cells were mostly epithelial cells [CD326 + /CD31-] and by confocal microscopy the absence of fibroblasts (supplemental Fig. 3). Ultrastructure of the TJ was revealed by *transmission electron microscopy* (supplemental Fig. 3A-C). Thus, fully differentiated, pseudostratified, ciliated HAE cells are predominantly bronchial epithelial cells.

Supplementary material related to this article can be found online at doi:10.1016/j.addma.2020.101681.

3.1.1. Inoculation of pneumococci results in stable apical colonisation at 6 h

To resemble natural lung infection where nutrients are acquired by Spn from human cells, i.e., instead from the cell culture medium, BSS was added to the apical side of differentiated HAE cells before infecting the cells with wtSpn or the Δ*comC* mutant. Colonising Spn at the apical side reached a plateau and the highest density ($\sim 10^{10}$ cfu/ml) within 6 h of incubation after which there was no further increase (Fig. 3A, B, C). In contrast, Spn was cultured in low frequency from the basolateral side (translocation, “invasive disease”) at this time point at any of the utilised inocula (Fig. 3D).

Three-dimensional (3D) reconstruction of confocal z-stacks and analysis of orthogonal zy planes demonstrated Spn on the apical side of differentiated HAE cells (i.e., above the TJ staining) (Fig. 2A, arrow). Spn formed microcolonies particularly colocalising with cilia (Figs. 2A, 2B, arrow). Dotted cilia were noticed in areas where Spn colonised HAE cells suggesting that bacteria had degraded cilia (Fig. 2 A-F, arrows).

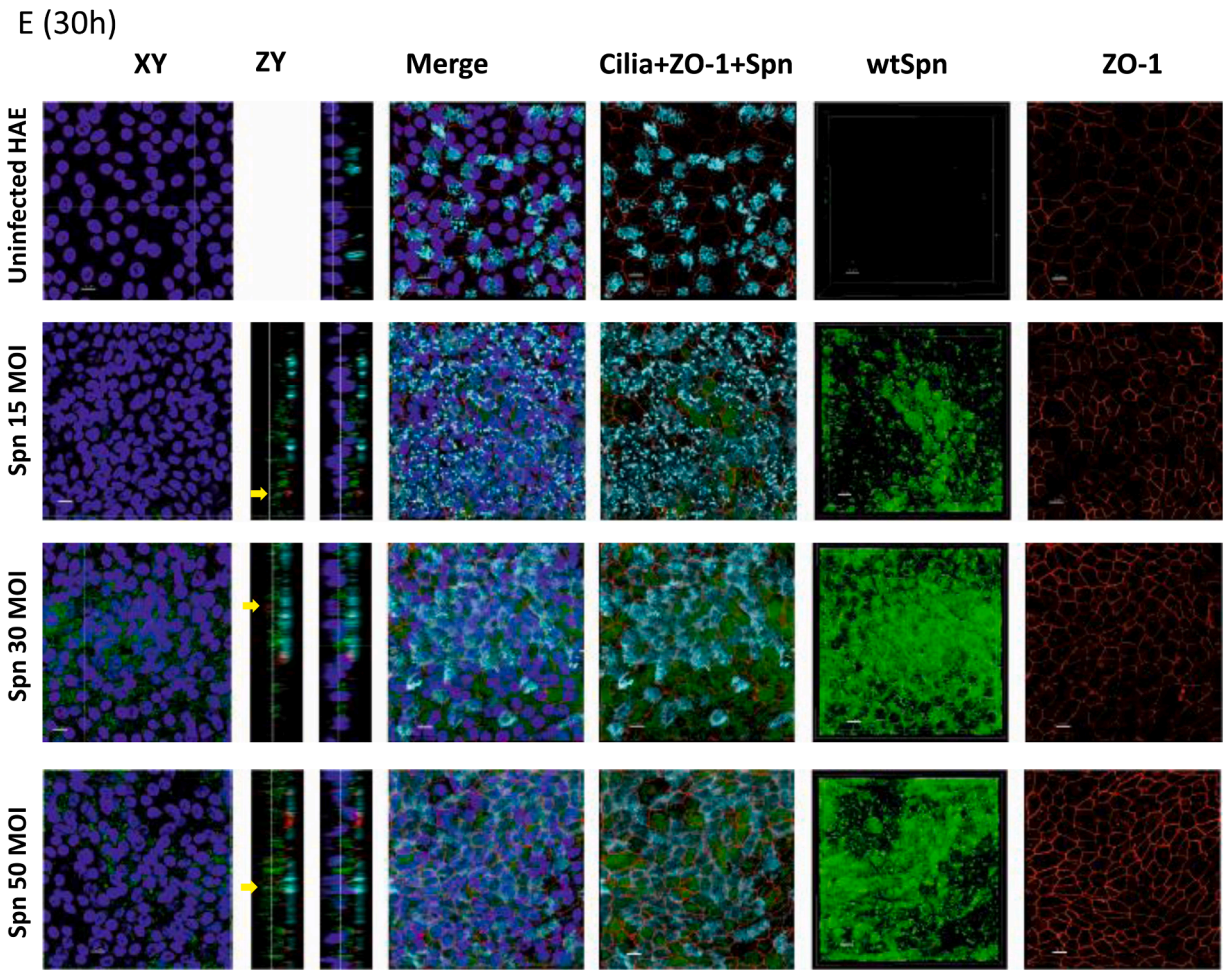

Fig. 2. (*continued*).

Taken together, this suggests that at 6 h post-inoculation, pneumococci were mainly attached on top of HAE cells, representing colonisation.

3.2. Loss of com quorum sensing induces a disorganised adhesion phenotype with translocation to the basolateral side

An important role of the Com QS system is to provide extracellular DNA (eDNA) during colonisation, a response mediated by a density threshold. We therefore assessed the adhesion phenotype and translocation of the isogenic Δ*comC* mutant strain. At 19 h post-inoculation there was a trend for increasing apical Spn densities with increasing doses whereas this trend was not seen after 30 h suggesting steady state of colonisation after 6 h (Fig. 3 A-C). Compared to wtSpn, the Δ*comC* colonised significantly less at 6 h post-inoculation but at higher levels at 19 h and 30 h (Fig. 3 A-C). In contrast, more Δ*comC* than wtSpn translocated at 6 h. Compared to 6 h, there was an increased number of Spn identified at the basolateral side at 19 h and 30 h with higher counts for wtSpn (Fig. 3 D-F).

In confocal imaging, there was prominent microcolony formation with wtSpn on top of HAE cells at 19 h and 30 h compared to increasing disintegration of microcolony structures over time with Δ*comC* (Fig. 2 C-F). zy confocal sections revealed the colocalisation of intracellular Spn with both cilia and ZO-1 at all time points (transmigration, Fig. 2 C-F, yellow arrows). These experiments suggest that pneumococcus primarily attaches to ciliated structures to gain access to human lung cells (Figs. 2A, 2B, yellow arrows). Translocation to the basolateral side increased from 6 h to 19–30 h post-inoculation correlating inversely with colonisation density.

3.3. Pneumococcal translocation correlates with a decreased transepithelial electrical resistance, that is specific and depends on time and dose of Spn

To begin studying the invasion mechanism, TEER was measured across HAE cells infected with TIGR4 as a correlate of the integrity of the TJ complex (Fig. 4A). Overall, a similar trend of decline was present over time, but with varying magnitude and timing. Starting TEERs ranged from 600 to 800 Ω/cm^2. There was a drop of median TEER at 6 h post-infection followed by a continued decrease. At 19 h post-infection, TEER had decreased by ~60% (Fig. 4A) and by ~85% at 28 h post-inoculation in comparison to the uninfected control (Fig. 4B). A similar time-dependent TEER decrease was observed when HAE cells were inoculated with a lower dose (Fig. 4B) or with another reference Spn strain (ATCC 49619, Fig. 4C). However, this decrease was specific for pneumococcal infection as it was different from TEER courses after incubation with latex particles (Fig. 4C) or with heat-killed wtSpn (supplemental Fig. 3) or BSS alone (0 MOI). Increasing inocula were associated with faster TEER decrease in wtSpn (r –0.81, $p = 0.002$; Fig. 4C). A time-course study revealed that TEER decreased earlier and more rapidly with the Δ*comC* mutant compared to wtSpn while levelling off at 19 h and at 30 h with steeper slopes for higher inocula. The strain had an effect on TEER over time showed, as indicated by a significant interaction of the two variables ($p < 0.001$). Indeed, TEER showed a faster decrease with Δ*comC* with a significant TEER difference at 6 h, but

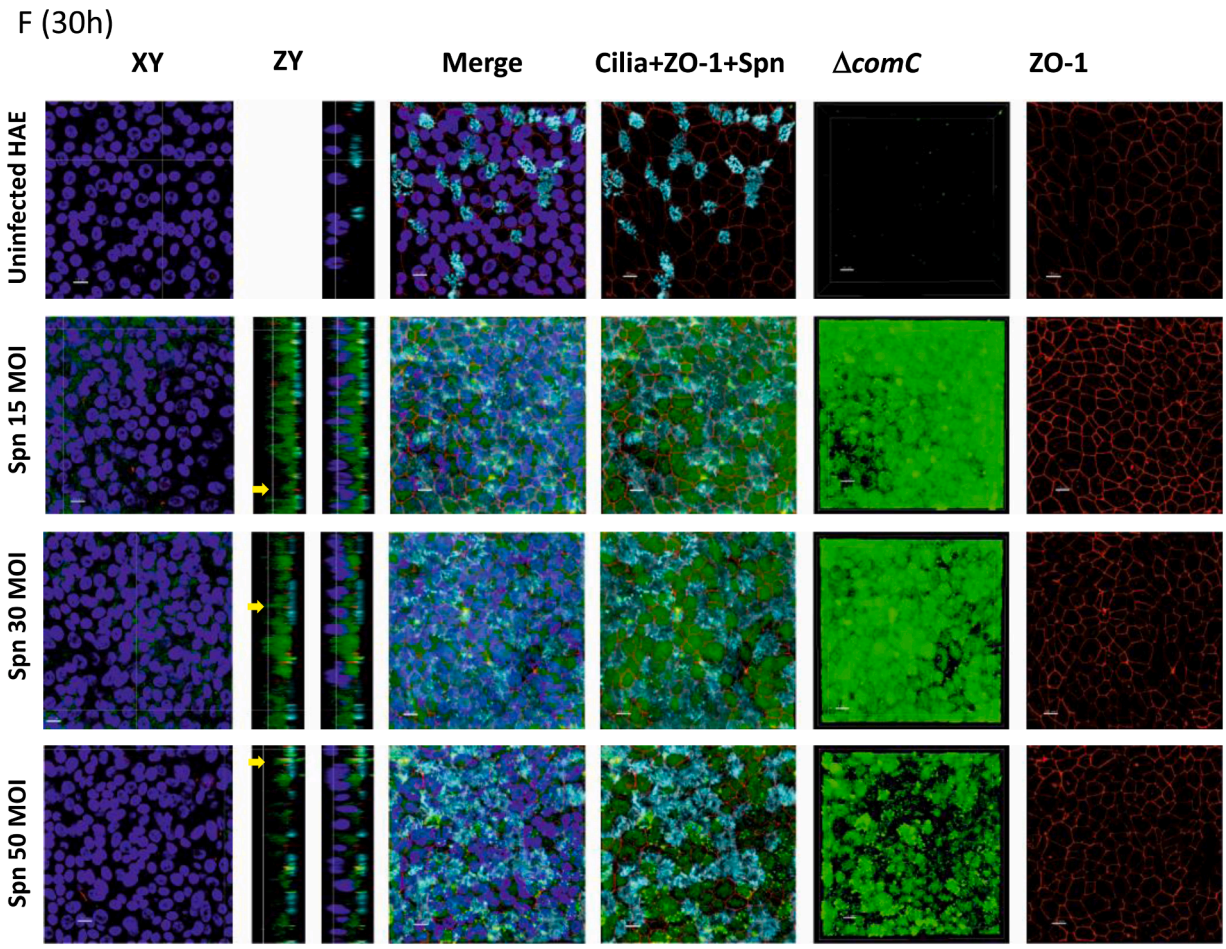

Fig. 2. (*continued*).

not at 19 h and 30 h ($p = 0.01$, $p = 0.18$ and $p = 0.15$, respectively; Fig. 4D). Thus, periods with steeper TEER decrease correlated with periods of increased translocation (Fig. 3D-F).

3.4. Pneumococcal translocation is not induced by cytotoxicity

To evaluate whether translocation of pneumococci was due to cytotoxicity, lactate dehydrogenase (LDH) release in the supernatant was measured after inoculation of HAE cells with wtSpn or Δ*comC*. LDH levels were similar 6 h post-inoculation with both strains but significantly higher with Δ*comC* after 19 h and 30 h of incubation (Fig. 5A). For both wtSpn and Δ*comC*, LDH levels significantly increased with longer incubation (Fig. 5A). Higher LDH levels were observed with Δ*comC* mutant compared to wtSpn for all inoculation doses (Fig. 5B). When there was no translocation, LDH levels did not differ between both strains until 19 h but were higher with Δ*comC* after 30 h (Fig. 5C). With translocation, higher LDH levels were seen with Δ*comC* compared to wtSpn at 19 h and 30 h (Fig. 5D). Surprisingly, among wtSpn, inserts with translocation showed significantly lower LDH levels at 19 h and 30 h than those without translocation (Fig. 5E). In contrast, among Δ*comC*, LDH levels were similar regardless of translocation (Fig. 5F).

Spn also produces a homolog LDH enzyme during its metabolism (Gaspar et al., 2014). We therefore quantified the amount of LDH in cultures of wtSpn grown for up to 30 h and LDH levels were below the limit of detection (15 U/L).

Collectively, this indicates higher cytotoxicity by infection with Δ*comC* mutant than wtSpn which does not correspond to periods of increased translocation. Therefore, cytotoxicity is likely not the mechanism leading to translocation.

3.5. Inoculation of HAE cells with pneumococci results in disintegration of the TJ

Since intracellular pneumococci colocalised with ZO-1 staining, we quantified the release of ZO-1 into the supernatants using ELISA. ZO-1 levels were significantly higher in HAE cells infected with Δ*comC* mutant than wtSpn ($p < 0.0001$; Figs. 6A, 6B). ZO-1 levels increased over time, particularly in HAE cells infected with Δ*comC* (Fig. 6B) but were independent of inoculum density (Fig. 6C) and were not linked to translocation (Fig. 6D).

To investigate whether ZO-1 in the supernatant was released from damaged HAE cells or resulted from upregulated gene expression, ZO-1 mRNA was measured in infected HAE cells. Lower ZO-1 transcription levels were detected in HAE cells infected with Δ*comC* mutant than with wtSpn (supplemental Fig. 5A). This became apparent at 19 h and was significant at 30 h post-infection (supplemental Fig. 5B), but without a dose-response effect (supplemental Fig. 5C). There was a non-significant trend for downregulation of ZO-1 expression in inserts with translocation compared to those without translocation, both for wtSpn and Δ*comC* (supplemental Fig. 5).

Overall, these results confirm that increased ZO-1 levels in supernatant cannot be attributed to increased ZO-1 expression but rather to increased release of ZO-1 into the supernatant.

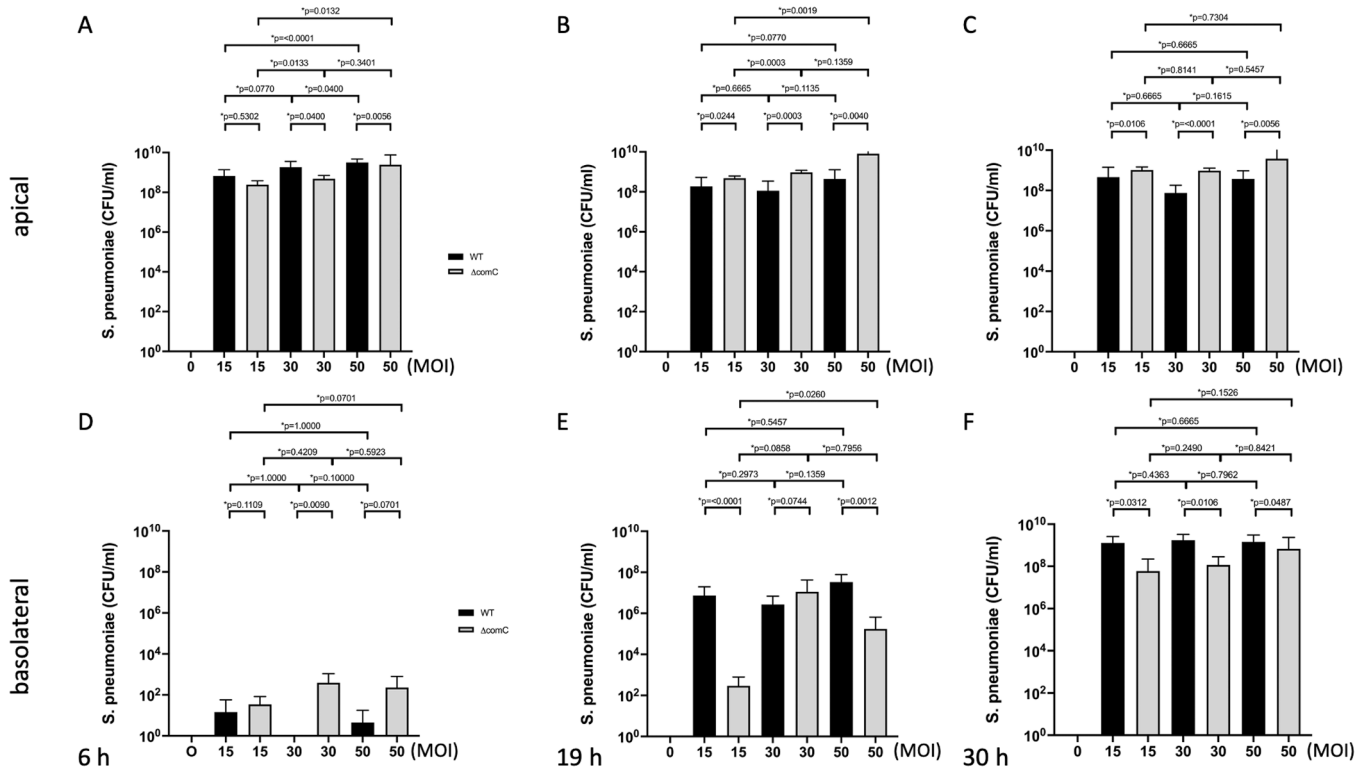

Fig. 3. Quantification of Streptococcus pneumoniae colonisation of and translocation. Pneumococci were infected at the apical side of differentiated HAE cells at a multiplicity of infection (MOI) of 15, 30 and 50. The density of bacteria in the apical and basolateral space was obtained by dilution and plating (CFU) at 6 h, 19 h and 30 h post-inoculation.

3.6. Temporal expression of specific host cytokines reflects colonisation and translocation

Secretion of 42 different human cytokines was evaluated during colonisation and translocation in the supernatants of HAE cells inoculated with pneumococci in comparison to either uninfected HAE control cells or wtSpn infected cells versus those infected with Δ*comC*. Remarkably, compared to non-infected cells, at the initial colonisation stage only IL-18 was significantly increased by ~60-fold in HAE cells infected with wtSpn and Δ*comC* mutant (Fig. 7A-7E). Additional cytokines were downregulated by the infection with the Δ*comC* mutant compared to that of wtSpn, including IL-13, and platelet-derived growth factor (PDGF) (Fig. 7F). Furthermore, in HAE cells infected with the Δ*comC*, levels of IL-18 were significantly increased at 19 h and 30 h post-infection (Figs. 7B and 7C) compared to the 6 h colonisation stage, whereas there was no further increase for wtSpn beyond 6 h (Figs. 7B, 7C, 7E and 7F).

Infection with wtSpn did not consistently induce a significant change in the secretion of other cytokines at 6 h and 19 h, in comparison to the uninfected control. Only at 30 h post-infection, secretion of IL-8 and epidermal growth factor was significantly increased at all inoculated densities (Fig. 7D). In contrast, whether compared against the uninfected control or against cytokine production by cells infected with wtSpn, differentiated HAE cells infected with Δ*comC* mutant had significantly higher levels of G-CSF at 19 h post-infection and at 30 h increased levels of IL-1α, IL-1RA, IL-1β, IL-4, IL-8, IL-9, TNF-α, and significantly decreased detection of several cytokines including IL-3, IL-7 and RANTES (Figs. 7E and 7F). Overall, we identified a signature of cytokine production in response to the absence of the competence stimulating peptide.

Together, our data reveal an increased cytotoxic phenotype upon inactivation of *com* quorum sensing signalling.

4. Discussion

This differentiated HAE model simulates the entire pathway from pneumococcal colonisation of human lower airways to transepithelial migration and IPD. Cultures from the basolateral space revealed an infectious dose- and time-dependent penetration through the respiratory epithelium accompanied by an epithelial response. Confocal imaging demonstrated co-localisation of pneumococci with TJ and cilia and subsequent degradation of ciliary and TJ structures. Translocation into the basolateral space coincided with loss of epithelial integrity as shown by a TEER decrease. The host response to pneumococcal invasion was characterised by an increase of proinflammatory cytokines but it was altered when the *com* QS system was inactivated. Our model suggests that Com is associated with microcolony formation during colonisation and translocation, whereas inactivation of *comC*-mediated signalling correlates with epithelial disruption with increased cytotoxicity and an increased inflammatory response.

The Com pathway is a well-studied QS system. It allows bacterial intercellular communication and enables fratricide, uptake of exogenous DNA and genetic recombination (Prudhomme et al., 2016; Vidal et al., 2013a). *comC* encodes the competence stimulating peptide (CSP) that activates the QS system. Its inactivation results in vitro in a decreased production of early stages of biofilms (Trappetti et al., 2011; Vidal et al., 2013a).

Likewise, in the current study, inactivation of *comC* led to early reduced and disorganised pneumococcal colonisation along with increased cytotoxicity and upregulated cytokine response but impaired later transmigration. This is consistent with loss of a highly orchestrated host-pathogen interaction. Microinvasion was followed by an inflammatory response which was postulated as a mechanism for subsequent pneumococcal clearance (Weight et al., 2019). Given the increased identification of hormones and molecules that block bacterial QS

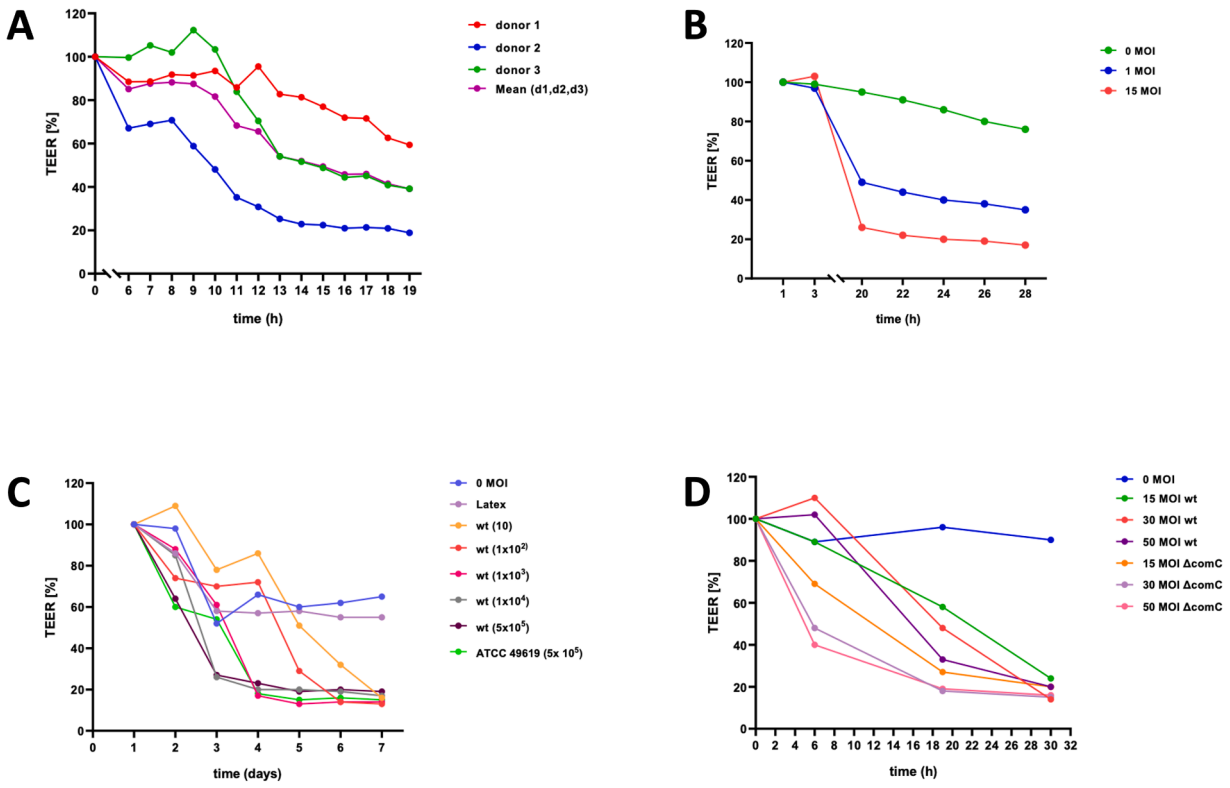

Fig. 4. Quantification of transepithelial electrical resistance of differentiated HAE cells infected with Streptococcus pneumoniae. Differentiated HAE cells were infected with wtSpn at 15 MOI from 3 donors. The transepithelial electrical resistance (TEER) was obtained every hour between 6 h through 19 h post-infection (A). HAE cells were infected with wtSpn at 0, 1, or 15 MOI and TEER was evaluated at the indicated time points (B). HAE cells were infected with different pneumococcal strains (wt-TIGR4, ATCC 49619) at different concentrations or mock infected with buffer or latex particles. TEER was evaluated every day (i.e., 24 h) post-infection for 7 days (C). TEER was measured at different time points post-infection with wtSpn or TIGR4 Δ*comC* mutant at different concentrations (D). Baseline TEER prior to infection was set to 100%. Changes of TEER are shown as percentage of decrease considering the baseline TEER maximum (100%) resistance (A-D).

systems, it is likely that blocking *com*-QS may modulate severe cases of human pneumococcal disease. This potential mechanism is under investigation in our laboratories.

Upregulation of proinflammatory cytokines correlated with cytotoxicity. For example, levels of both IL-18 and LDH were increased in those HAE cells infected with Δ*comC* mutant compared to uninfected cells and with those infected with the wtSpn. The release of activated IL-18 and IL-1β is a hallmark of canonical -caspase-1-dependent- activation of the NLRP3 inflammasome (Surabhi et al., 2020). Cell death can occur by uncontrolled activation of the NLRP3 inflammasome, known as pyroptosis (Jing et al., 2021; Ta and Vanaja, 2021). IL-18 has both IFNγ-dependent and –independent proinflammatory activity (Novick et al., 2013). Therefore, evidence from this model indicates that pneumococci elicit a distinct IL-18 mediated inflammatory response that can induce differentiated human lung cells to undergo pyroptosis, particularly when *com*-QS is inactivated. Both hydrogen peroxide and the pneumolysin (Ply) have been involved in triggering pyroptosis of in vitro cultured human bronchial cells (Karmakar et al., 2015; Surabhi et al., 2022) and in murine neutrophils. The genes encoding Ply (*ply*) and *spxB*, encoding an enzyme responsible for most hydrogen peroxide, are upregulated when Spn infects human lung cells(Aprianto et al., 2018). Our data showed no difference in hydrogen peroxide production between wtSpn and Δ*comC* mutant. Interestingly, inactivation of *comC* was associated with an increased expression of the pore-forming and pro-inflammatory pneumolysin, an observation which to our knowledge has not been reported yet, and which is subject to further investigation in our laboratories. In contrast, a *luxS* mutant for a different pneumococcal quorum sensing system was previously shown to have reduced *pneumolysin* gene expression (Joyce et al., 2004). Because the HAE model has unique characteristics not present in immortalized lung cells, the possibility exists that other unknown molecules are expressed when infecting HAE cells and contribute to the exacerbated activation of the inflammasome. Our laboratories are exploring this possibility as well.

Except for immortalised cell cultures and animal models, we are aware of only three published lung tissue models (Marks et al., 2012; Szymanski et al., 2012; Weight et al., 2019). The first model used a lung mucoepidermoid carcinoma cell line (NCI-H292) or paraformaldehyde-fixed primary differentiated tracheobronchial epithelial cells from healthy volunteers to study pneumococcal biofilms (Marks et al., 2012). A second model investigated infection on fresh lung tissue cylinders. In contrast, in our model bronchial epithelial cells are harvested to a single cell suspension that allows cryopreservation and stocking cells for repeated experiments. A third model describes an experimental human pneumococcal carriage model and in addition a HAE model that recapitulated in vivo findings (Weight et al., 2019). This epithelial model is very similar to ours. Importantly and confirming the applicability of our HAE model to in vivo situations, Weight et al. also reported adhesion, microcolony formation and epithelial invasion of a serotype 6B pneumococcus. This model focussed on the first 3 h of pneumococcal infection whereas we studied infection for up to 30 h.

There are several major strengths of our experimental setup which make it more physiologic compared to traditional cell cultures. First, we used a more realistic *ex vivo* model with differentiated cells. Secondly, pneumococci were inoculated on the apical side in the absence of cell culture medium. Consequently, bacteria acquired nutrients directly from their interaction with differentiated HAE cells. Unlike homogenous colonisation on the cell substrate seen in models where bacteria are inoculated in cell culture medium, in our model, colonising

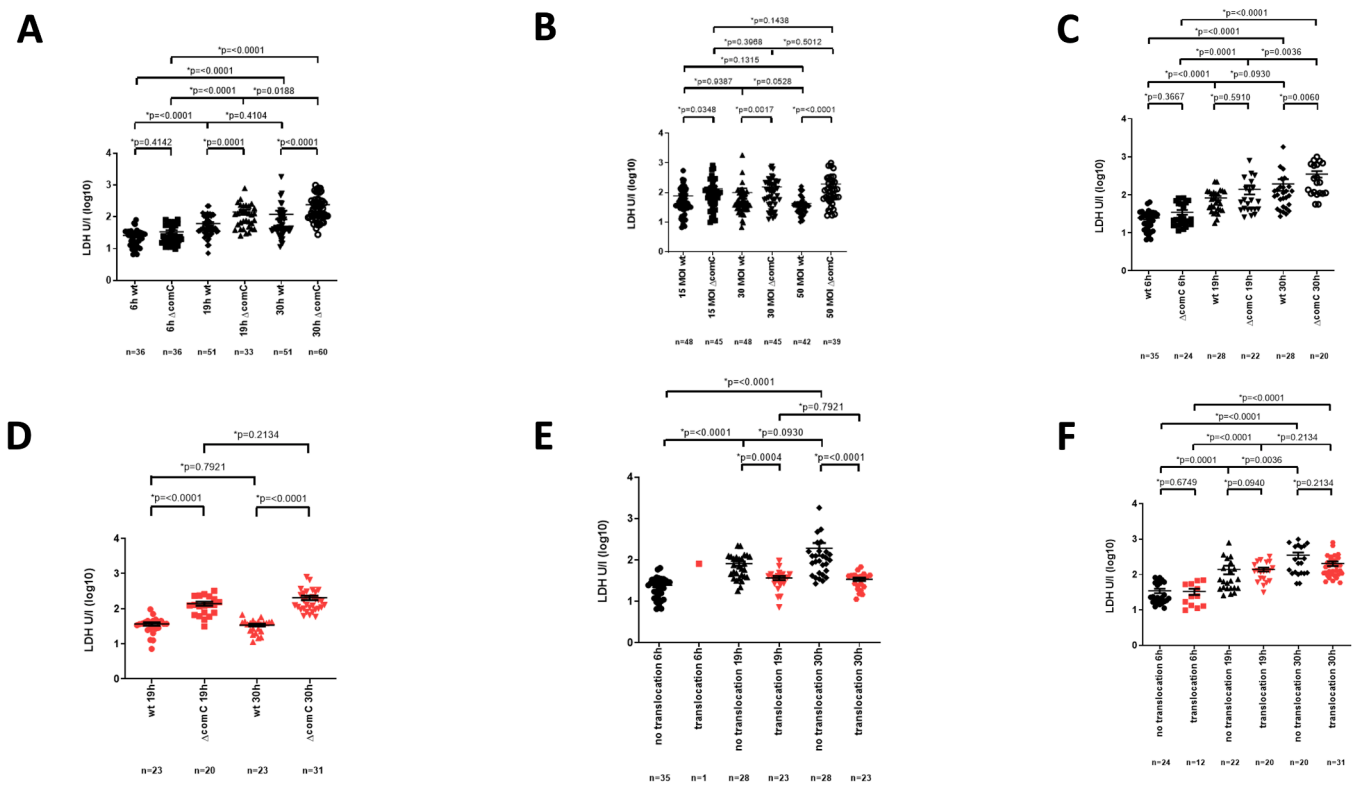

Fig. 5. Determination of cytotoxicity as measured by LDH in supernatant after pneumococcal infection. Lactate dehydrogenase (LDH) release was quantified (U/l) in supernatants of differentiated HAE cells, harvested from three different donors and inoculated with wtSpn or Δ*comC* mutant. LDH release after infection for different time points (A) and different concentrations (MOI) of wtSpn and Δ*comC* (B). LDH release is shown for infection with both strains in inserts without (C) and with (D) translocation at different time points. LDH release from cells is shown for inserts without and with translocation from HAE cells infected with wtSpn (E) and Δ*comC* mutant (F).

Error bars represent the standard errors of the means calculated using data from five independent experiments, that used HAE cells from three different donors and that included several transwell inserts in each biological replicate. Inserts with translocated bacteria are indicated in red, inserts without translocated bacteria in black (panel C-F). The total number (n) of transwell inserts with differentiated HAE cells tested is indicated under each strain/condition. *p*-values are shown on top of each comparison. *Indicates statistical significance $p < 0.05$.

pneumococci formed microcolonies. Similarly, Trappetti et al. also reported that a wtSpn strain formed microcolonies whereas the isogenic Δ*comC* mutant was unable to attach (Trappetti et al., 2011). Our *ex vivo* model indicated a loss of microcolony formation over time with a disorganised adhesion pattern in those infected with an inactivated *comC* system. Third, epithelium and response to infection is donor specific. Results that are generally reproducible with different human donors can thus be generalised. Donor-specificity is a great asset as this model reflects the individual physiological situation and susceptibility to colonisation and infection more closely than artificial systems or immortalised cell lines. Limitations of our HEA model include the lack of an adaptive immune response and the time required for epithelial differentiation.

In conclusion, our experiments indicate that the *com*C system allows a higher organisational level of population structure resulting in microcolony formation, increased early colonisation and subsequent translocation. We propose that inactivation of QS unleashes a very different and possibly more virulent phenotype of pneumococci that merits further investigation. This finding was observed using an *ex vivo* primary HAE model that recapitulates pathophysiological events of pneumococcal colonisation and invasion. It may thus allow identification of novel mechanisms to improve diagnostics and determine new preventive and therapeutic targets to combat pneumococcal diseases.

Funding

Work in the Vidal laboratory was in part supported by grants from the National Institutes of Health (NIH; 1R21AI144571-01, and 1R21AI151571-01A1). The content of the study is solely the responsibility of the authors and does not necessarily represent the official view of the NIH.

Work at the experimental infectiology laboratory at the Cantonal Hospital of St. Gallen was supported by the Lungenliga St. Gallen and funds of the Division of Infectious Diseases & Hospital Epidemiology, Cantonal Hospital St.Gallen.

The study received support through a grant from the Research Committee of the Kantonsspital St.Gallen (Grant number MFZF_2014-002).

CRediT authorship contribution statement

CRK and WCA initiated the study. CRK, WCA and JEV developed the design and methods. SN performed all experiments with exception of transmission electron microscopy, which was performed by LD and the haemoglobin release assays that was performed by AV. LO supervised confocal microscopy. CRK, SN, JEV and WCA performed statistical analyses. CRK, JEV and WCA wrote the manuscript. CRK, WCA, JEV, SN and LO contributed to data acquisition and interpretation. All authors revised and approved the manuscript for intellectual content. CRK, JEV and WCA had full access to the data in the study, all authors agreed to

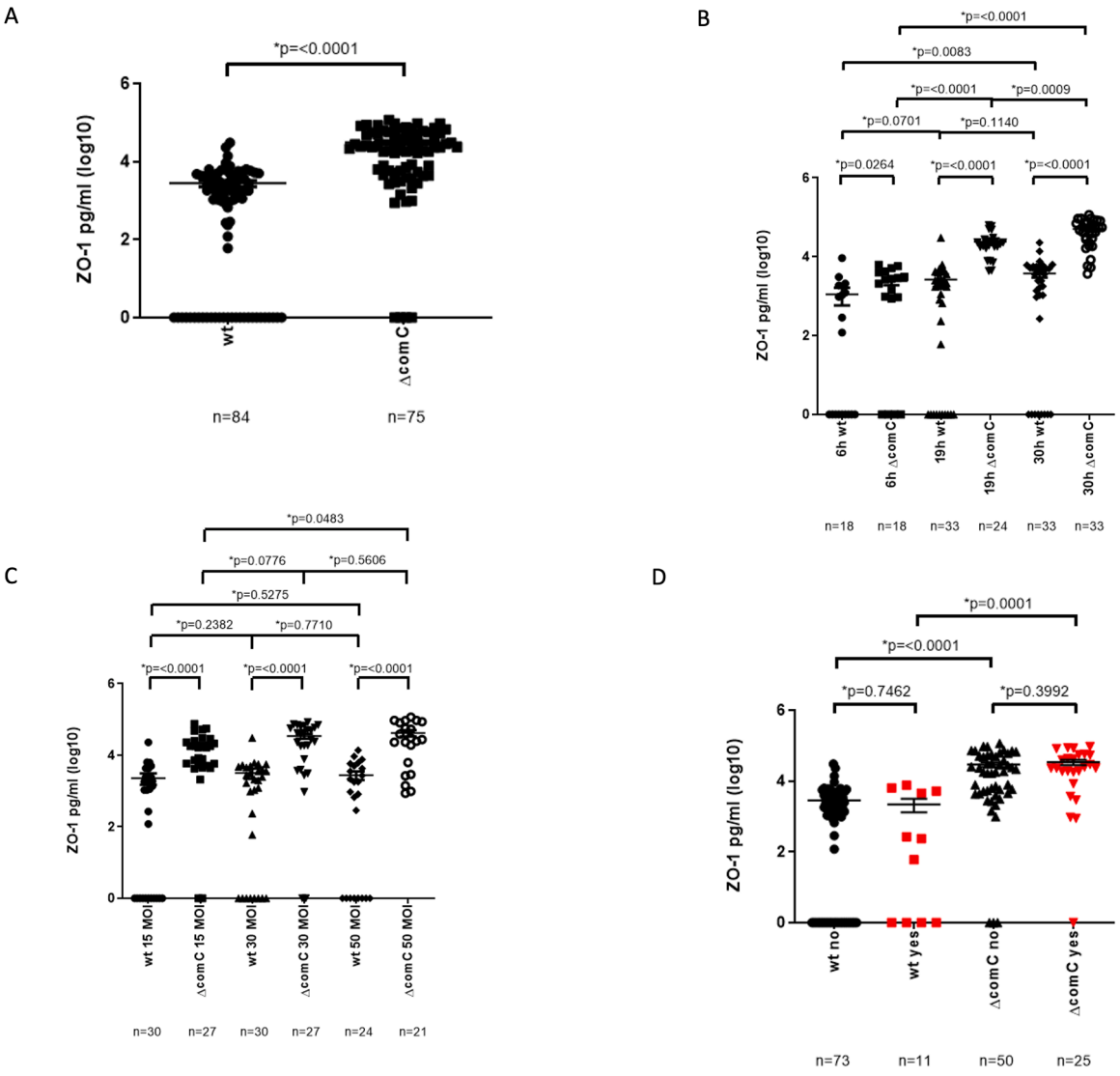

Fig. 6. Quantification of ZO-1 in the supernatant of epithelial cells after pneumococcal infection. ZO-1 release was quantified in supernatants of differentiated HAE cells harvested from two donors with wtSpn and Δ*comC* mutant at different concentrations (15, 30, or 50 MOI) and different time points (6 h, 19 h and 30 h) corrected for background values (0 MOI). ZO-1 levels are depicted in pg/ml after infection of HAE cells with wtSpn and Δ*comC* mutant overall (A), for different time points (B) and concentrations (C) and stratified for both strains each without translocation ("no") and with translocation ("yes") (D).

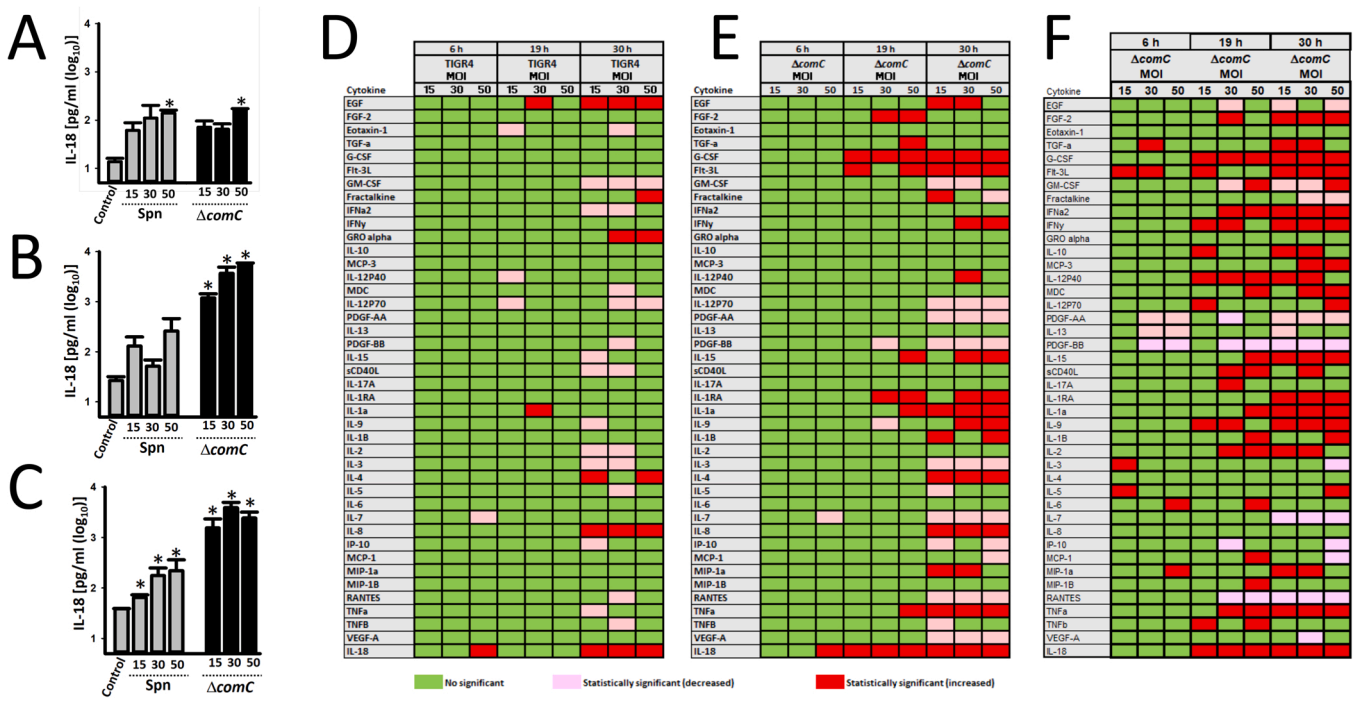

Fig. 7. Quantification of cytokine levels in the supernatant of airway epithelial cells after pneumococcal infection. Cytokines levels were measured in supernatant from HAE cells with different multiplicity of infection (MOI=15, 30, or 50) of wtSpn or ΔcomC mutant and incubated for 6 h, 19 h or 30 h. IL-18 levels post-infection are shown at 6 h (A), 19 h (B) or 30 h (C). *$p < 0.05$ refers to statistical significance versus IL-18 levels of supernatants of the uninfected control. Color coding of boxes indicates significantly ($p < 0.05$) increased (red) or decreased (pink) of the cytokine levels in the supernatant with wtSpn (D) or ΔcomC mutant (E) compared to the uninfected control and comparison wtSpn versus ΔcomC mutant (F). Green boxes refer to similar cytokine level as compared to the uninfected control.

the final version including submission for publication and accept responsibility for this work.

Conflict of interest

No potential conflicts of interest.

Data Availability

Data will be made available on request.

Acknowledgement

We sincerely thank Sabine Güsewell, PhD, for expert statistical advice, Christian Perez Shibayama, PhD, for support with flow cytometry and the reviewers for their constructive input.

Appendix A. Supporting information

Supplementary data associated with this article can be found in the online version at doi:10.1016/j.micres.2022.127297.

References

Albrich, W.C., Madhi, S.A., Adrian, P.V., van Niekerk, N., Mareletsi, T., Cutland, C., Wong, M., Khoosal, M., Karstaedt, A., Zhao, P., Deatly, A., Sidhu, M., Jansen, K.U., Klugman, K.P., 2012. Use of a rapid test of pneumococcal colonization density to diagnose pneumococcal pneumonia. Clin. Infect. Dis. 54, 601–609. https://doi.org/10.1093/cid/cir859.

Aprianto, R., Slager, J., Holsappel, S., Veening, J.-W., 2018. High-resolution analysis of the pneumococcal transcriptome under a wide range of infection-relevant conditions. Nucleic Acids Res. 46, 9990–10006. https://doi.org/10.1093/nar/gky750.

Bogaert, D., De Groot, R., Hermans, P.W.M., 2004. Streptococcus pneumoniae colonisation: the key to pneumococcal disease. Lancet Infect. Dis. 4, 144–154. https://doi.org/10.1016/S1473-3099(04)00938-7.

Boix-Palop, L., Obradors, M., Xercavins, M., Picó-Plana, E., Canales, L., Dietl, B., Pérez, J., Garau, J., Calbo, E., 2021. Improvement of pneumococcal pneumonia diagnosis using quantitative real-time PCR targeting lytA in adult patients: a prospective cohort study, 00300–1 Clin. Microbiol. Infect. S1198–743X (21). https://doi.org/10.1016/j.cmi.2021.05.049.

Carr, O.J.J., Vilivong, K., Bounvilay, L., Dunne, E.M., Lai, J.Y.R., Chan, J., Vongsakid, M., Chanthongthip, A., Siladeth, C., Ortika, B., Nguyen, C., Mayxay, M., Newton, P.N., Mulholland, K., Do, L. a, Dubot-Pérès, H., Satzke, A., Dance, C., D. a, B., Russell, F. M., 2021. Nasopharyngeal pneumococcal colonization density is associated with severe pneumonia in young children in the Lao PDR. J. Infect. Dis. https://doi.org/10.1093/infdis/jiab239.

Chiavolini, D., Pozzi, G., Ricci, S., 2008. Animal models of Streptococcus pneumoniae disease. Clin. Microbiol. Rev. 21, 666–685. https://doi.org/10.1128/CMR.00012-08.

Dijkman, R., Jebbink, M.F., Koekkoek, S.M., Deijs, M., Jónsdóttir, H.R., Molenkamp, R., Ieven, M., Goossens, H., Thiel, V., Hoek, L. van der, 2013a. Isolation and characterization of current human coronavirus strains in primary human epithelial cell cultures reveal differences in target cell tropism. J. Virol. 87, 6081. https://doi.org/10.1128/JVI.03368-12.

Dijkman, R., Jebbink, M.F., Koekkoek, S.M., Deijs, M., Jónsdóttir, H.R., Molenkamp, R., Ieven, M., Goossens, H., Thiel, V., Hoek, L. van der, 2013b. Isolation and characterization of current human coronavirus strains in primary human epithelial cell cultures reveal differences in target cell tropism. J. Virol. 87, 6081–6090. https://doi.org/10.1128/JVI.03368-12.

Felice, M.E., Shragg, G.P., James, M., Hollingsworth, D.R., 1987. Psychosocial aspects of Mexican-American, white, and black teenage pregnancy. J. Adolesc. Health Care 8, 330–335. https://doi.org/10.1016/0197-0070(87)90004-0.

Fulcher, M.L., Gabriel, S., Burns, K.A., Yankaskas, J.R., Randell, S.H., 2005. Well-differentiated human airway epithelial cell cultures. Methods Mol. Med. 107, 183–206. https://doi.org/10.1385/1-59259-861-7:183.

Ganaie, F., Saad, J.S., McGee, L., van Tonder, A.J., Bentley, S.D., Lo, S.W., Gladstone, R. A., Turner, P., Keenan, J.D., Breiman, R.F., Nahm, M.H., 2020. A new pneumococcal capsule type, 10D, is the 100th serotype and has a large cps fragment from an oral streptococcus. mBio 11, e00937. https://doi.org/10.1128/mBio.00937-20.

Gaspar, P., Al-Bayati, F.A.Y., Andrew, P.W., Neves, A.R., Yesilkaya, H., 2014. Lactate dehydrogenase is the key enzyme for pneumococcal pyruvate metabolism and pneumococcal survival in blood. Infect. Immun. 82, 5099–5109. https://doi.org/10.1128/IAI.02005-14.

Gritzfeld, J.F., Wright, A.D., Collins, A.M., Pennington, S.H., Wright, A.K.A., Kadioglu, A., Ferreira, D.M., Gordon, S.B., 2013. Experimental human pneumococcal carriage. J. Vis. Exp. 50115. https://doi.org/10.3791/50115.

Hocke, A.C., Suttorp, N., Hippenstiel, S., 2017. Human lung ex vivo infection models. Cell Tissue Res. 367, 511–524. https://doi.org/10.1007/s00441-016-2546-z.

Jing, W., Lo Pilato, J., Kay, C., Man, S.M., 2021. Activation mechanisms of inflammasomes by bacterial toxins. Cell. Microbiol. 23, e13309 https://doi.org/10.1111/cmi.13309.

Joyce, E.A., Kawale, A., Censini, S., Kim, C.C., Covacci, A., Falkow, S., 2004. LuxS is required for persistent pneumococcal carriage and expression of virulence and biosynthesis genes. Infect. Immun. 72, 2964–2975. https://doi.org/10.1128/IAI.72.5.2964-2975.2004.

Karmakar, M., Katsnelson, M., Malak, H.A., Greene, N.G., Howell, S.J., Hise, A.G., Camilli, A., Kadioglu, A., Dubyak, G.R., Pearlman, E., 2015. Neutrophil IL-1β processing induced by pneumolysin is mediated by the NLRP3/ASC inflammasome and caspase-1 activation and is dependent on K+ efflux. J. Immunol. 194, 1763–1775. https://doi.org/10.4049/jimmunol.1401624.

Marks, L.R., Parameswaran, G.I., Hakansson, A.P., 2012. Pneumococcal interactions with epithelial cells are crucial for optimal biofilm formation and colonization in vitro and in vivo. Infect. Immun. 80, 2744–2760. https://doi.org/10.1128/IAI.00488-12.

Nikolaou, E., Jochems, S.P., Mitsi, E., Pojar, S., Blizard, A., Reiné, J., Solórzano, C., Negera, E., Carniel, B., Soares-Schanoski, A., Connor, V., Adler, H., Zaidi, S.R., Hales, C., Hill, H., Hyder-Wright, A., Gordon, S.B., Rylance, J., Ferreira, D.M., 2021. Experimental human challenge defines distinct pneumococcal kinetic profiles and mucosal responses between colonized and non-colonized adults. e02020-e02020 mBio 12. https://doi.org/10.1128/mBio.02020-20.

Novick, D., Kim, S., Kaplanski, G., Dinarello, C.A., 2013. Interleukin-18, more than a Th1 cytokine. Semin. Immunol. 25, 439–448. https://doi.org/10.1016/j.smim.2013.10.014.

Prudhomme, M., Berge, M., Martin, B., Polard, P., 2016. Pneumococcal competence coordination relies on a cell-contact sensing mechanism. PLoS Genet. 12, e1006113 https://doi.org/10.1371/journal.pgen.1006113.

Scott, J.R., Millar, E.V., Lipsitch, M., Moulton, L.H., Weatherholtz, R., Perilla, M.J., Jackson, D.M., Beall, B., Craig, M.J., Reid, R., Santosham, M., O'Brien, K.L., 2012. Impact of more than a decade of pneumococcal conjugate vaccine use on carriage and invasive potential in Native American communities. J. Infect. Dis. 205, 280–288. https://doi.org/10.1093/infdis/jir730.

Surabhi, S., Cuypers, F., Hammerschmidt, S., Siemens, N., 2020. The role of NLRP3 inflammasome in pneumococcal infections. Front. Immunol. 11, 614801 https://doi.org/10.3389/fimmu.2020.614801.

Surabhi, S., Jachmann, L.H., Shumba, P., Burchhardt, G., Hammerschmidt, S., Siemens, N., 2022. Hydrogen peroxide is crucial for NLRP3 inflammasome-mediated IL-1β production and cell death in pneumococcal infections of bronchial epithelial cells. J. Innate Immun. 14, 192–206. https://doi.org/10.1159/000517855.

Szymanski, K.V., Toennies, M., Becher, A., Fatykhova, D., N'Guessan, P.D., Gutbier, B., Klauschen, F., Neuschaefer-Rube, F., Schneider, P., Rueckert, J., Neudecker, J., Bauer, T.T., Dalhoff, K., Drömann, D., Gruber, A.D., Kershaw, O., Temmesfeld-Wollbrueck, B., Suttorp, N., Hippenstiel, S., Hocke, A.C., 2012. Streptococcus pneumoniae-induced regulation of cyclooxygenase-2 in human lung tissue. Eur. Respir. J. 40, 1458–1467. https://doi.org/10.1183/09031936.00186911.

Ta, A., Vanaja, S.K., 2021. Inflammasome activation and evasion by bacterial pathogens. Curr. Opin. Immunol. 68, 125–133. https://doi.org/10.1016/j.coi.2020.11.006.

Trappetti, C., Gualdi, L., Di Meola, L., Jain, P., Korir, C.C., Edmonds, P., Iannelli, F., Ricci, S., Pozzi, G., Oggioni, M.R., 2011. The impact of the competence quorum sensing system on Streptococcus pneumoniae biofilms varies depending on the experimental model. BMC Microbiol. 11, 75. https://doi.org/10.1186/1471-2180-11-75.

Trappetti, C., McAllister, L.J., Chen, A., Wang, H., Paton, A.W., Oggioni, M.R., McDevitt, C.A., Paton, J.C., 2017. Autoinducer 2 signaling via the phosphotransferase FruA drives galactose utilization by streptococcus pneumoniae, resulting in hypervirulence. e02269-16 mBio 8. https://doi.org/10.1128/mBio.02269-16.

Vidal, J.E., Howery, K.E., Ludewick, H.P., Nava, P., Klugman, K.P., 2013a. Quorum-sensing systems LuxS/autoinducer 2 and Com regulate Streptococcus pneumoniae biofilms in a bioreactor with living cultures of human respiratory cells. Infect. Immun. 81, 1341–1353. https://doi.org/10.1128/IAI.01096-12.

Vidal, J.E., Howery, K.E., Ludewick, H.P., Nava, P., Klugman, K.P., 2013b. Quorum-sensing systems LuxS/autoinducer 2 and Com regulate Streptococcus pneumoniae biofilms in a bioreactor with living cultures of human respiratory cells. Infect. Immun. 81, 1341–1353. https://doi.org/10.1128/IAI.01096-12.

Weight, C.M., Venturini, C., Pojar, S., Jochems, S.P., Reiné, J., Nikolaou, E., Solórzano, C., Noursadeghi, M., Brown, J.S., Ferreira, D.M., Heyderman, R.S., 2019. Microinvasion by Streptococcus pneumoniae induces epithelial innate immunity during colonisation at the human mucosal surface. Nat. Commun. 10, 3060. https://doi.org/10.1038/s41467-019-11005-2.

Welte, T., Torres, A., Nathwani, D., 2012. Clinical and economic burden of community-acquired pneumonia among adults in Europe. Thorax 67, 71–79. https://doi.org/10.1136/thx.2009.129502.

Wright, A.K.A., Bangert, M., Gritzfeld, J.F., Ferreira, D.M., Jambo, K.C., Wright, A.D., Collins, A.M., Gordon, S.B., 2013. Experimental human pneumococcal carriage augments IL-17A-dependent T-cell defence of the lung. PLoS Pathog. 9, e1003274 https://doi.org/10.1371/journal.ppat.1003274.